trajectories were calculated. These computations used identical sets of initial conditions, and a trim angle of 60° with either continuum aerodynamics or low Reynolds number aerodynamics. For the continuum case, a lift-drag ratio of 0.5 was used for the entire trajectory; for the low Reynolds number case, the L/D was varied linearly from 0.26 at 400,000 ft altitude to 0.5 at 250,000 ft, and then kept constant for the remaining trajectory. The calculations were made for an azimuth angle of 32°, an Earth reference velocity of 25, 134 fps, and the lift vector in the positive vertical position (roll angle $\phi = 0°$) or inclined (roll angle $\phi = 45°$). The results of these computations are presented in Table 1. In all cases, the low density effects produce only minor changes in range, g loads, and maximum heating conditions.

In summary, lift and drag forces were measured on a typical SSV design in the hypersonic flow regime using a free-flight technique. Significant decreases in lift due to low Reynolds number effects were measured for this space shuttle vehicle. However, calculated entry trajectories are essentially the same whether or not these low density effects are taken into account.

References

[1] Faget, M., "Space Shuttle: A New Configuration," *Astronautics and Aeronautics*, Vol. 8, No. 1, Jan. 1970, p. 52.

[2] Horstman, C. C. and Kussoy, M. I., "Free-Flight Measurements of Aerodynamic Viscous Effects on Lifting Re-Entry Bodies," *Journal of Spacecraft and Rockets*, Vol. 4, No. 8, Aug. 1967, p. 1064.

[3] Kussoy, M. I. and Horstman, C. C., "Cone Drag in Rarefied Hypersonic Flow," *AIAA Journal*, Vol. 8, No. 2, Feb. 1970, p. 315.

[4] Geiger, R. E., "Slender Cone, Zero Angle of Attack Drag in Continuum and Noncontinuum Flow," AIAA Paper 69-711, San Francisco, Calif., 1969.

Drag of Vane-Type Vortex Generators in Compressible Flow

J. C. Westkaemper* and Jerry W. Whitten†
The University of Texas at Austin, Austin, Texas

Nomenclature

AR = aspect ratio
b = vortex generator span
b_r = generator trailing edge span
C_D = drag coefficient
C_f = skin-friction coefficient
C_p = pressure coefficient
c = generator chord length
D = drag force
d = leading edge thickness
l = wedge centerline length
M = Mach number
q = dynamic pressure
S = reference area
x = distance along wedge axis
θ = leading-edge sweep angle
α = angle of attack
δ = nominal boundary layer thickness
ϵ = rake angle
ϕ = wedge total angle
γ = ratio of specific heats

Subscripts

a = boundary-layer average
g = vortex generator
i = incompressible
n = leading-edge nose
w = wedge
∞ = freestream

Received June 11, 1970; revision received July 15, 1970. This work was sponsored by the Naval Air Systems Command, under Subcontract 181471 with the Applied Physics Laboratory of The Johns Hopkins University.

* Research Engineer and Associate Professor of Aerospace Engineering, Applied Research Laboratory. Associate Fellow AIAA.

† Research Engineer, Applied Research Laboratory; now with the Boeing Company, Seattle, Wash.

Introduction

THE use of vane-type vortex generators in subsonic flows is widespread. Boundary-layer separation can be delayed or prevented on aircraft wings and stabilizers, in jet-engine inlets and similar diffusers. There has been little use of the generators in the supersonic speed regime, however. This may be in part the result of the lack of information on their performance in compressible flow. Reference 1 reports the results of flight tests of generators used to control separation on a flapped wing on a missile, primarily at transonic speeds. Limited data at Mach numbers up to 1.35 indicated that some configurations improved and some degraded the wing performance. No systematic investigation was made, however. In Ref. 2, in tests of a supersonic inlet, the vortex generators were in supersonic flow for some test conditions; here they "continued to function properly" in improving pressure recovery. The maximum Mach number at the generator location was 1.45. Again no systematic study was made of generator configurations.

The present work is part of a wind-tunnel test program to determine the usefulness of vortex generators in preventing separation of turbulent, compressible boundary layers. This Note covers an investigation of the drag of vane-type generators. Vane planforms were limited to simple shapes, since no data were available to aid in predicting an optimum shape.

Apparatus and Procedure

The tests were made in a blowdown-type wind tunnel having test section dimensions of 6 × 7 in. with fixed nozzle blocks giving a test Mach number of 4.9. A stagnation temperature of 660 ± 5° R was used to preclude moisture condensation and air liquefaction. A stagnation pressure of 260 ± 5 psig was employed, resulting in an average freestream Reynolds number of 1.08 million/in.

The vortex generators were mounted on the flat plate shown in Fig. 1. This aluminum plate was 6 in. wide, 17.5 in. long, and 0.875 in. thick. The leading edge had a wedge angle of 14°. A half-in.-wide strip of 80-grit emery cloth was cemented to the test surface, ½ in. downstream of the leading edge, to serve as a boundary-layer trip. This resulted in a

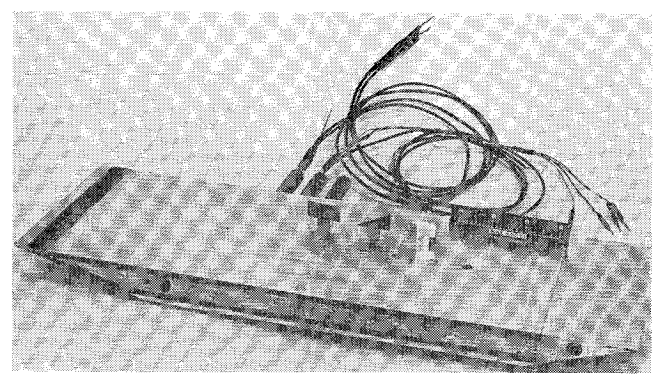

Fig. 1 Vortex generators and flat plate.

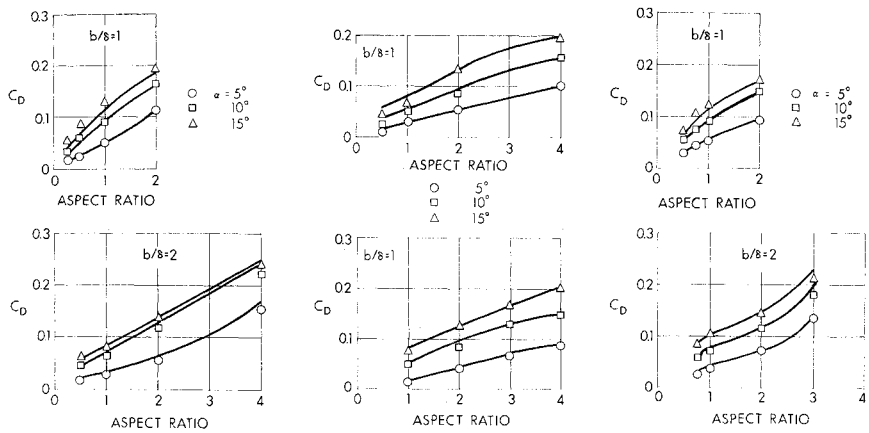

Fig. 2 Drag coefficient results.

a) Rectangular planform **b) Half-delta planform** **c) Raked-tip planform**

turbulent boundary layer ~0.25 in. thick at the generator test station, which was 9.5 in. from the plate leading edge. The test surface was aligned with the horizontal center plane of the nozzle. The plate instrumentation included static pressure taps and a thermocouple. The plate temperature was controlled by a heating element built into the plate body. The plate included a 1 in. diam hole at the test station in order to accommodate the drag balance.

The drag of each vortex generator was measured using a modified floating-element type drag balance.[3] The balance was installed in the plate with the generator-mounting disk flush with the plate surface, as seen in Fig. 1. The opening in the plate was 0.008 in. larger than the spring-supported disk, which was thus free to deflect ±0.004 in. in the airflow direction under the action of drag forces. Leaf springs of various stiffnesses were used as necessary. Figure 1 shows generators having planforms typical of those tested. Table 1 gives detailed dimensions of the entire series of generators, where the rectangular, half-delta and raked-tip rectangular planforms are denoted as configuration A, B, and C, respectively. Two generator spans per configuration were selected for testing; a $\frac{1}{4}$ in. span (equal to the nominal thickness of the boundary layer), and a $\frac{1}{2}$ in. span. For each span there were four generators of various aspect ratios, giving a total of eight sizes for each planform shape and 24 generators in the complete series. The vanes were machined from $\frac{1}{16}$ in. thick aluminum sheet. Each leading edge was a wedge of total angle of ~22°; all trailing edges were blunt. No hand finishing was employed since it was intended to have a finish typical of a production shop process. Each generator incorporated a rectangular tab protruding from its base in order to mount it in the corresponding slot in the drag-balance disk.

Prior to each run, the plate heating element was switched on to heat the plate and drag balance to the recovery temperature (125° F) corresponding to the predetermined stagnation temperature. The balance was then calibrated using a low-friction pulley and dead weights. At least two runs were made for each generator at angles of attack of 5°, 10°, and 15°. After the tests with generators were completed, several runs were made with a smooth disk, and this tare drag value was subtracted from the readings obtained for each generator. The apparatus and procedure are discussed in greater detail in Ref. 4.

Drag Calculations

For the drag calculations, the boundary layer was treated as a region of uniform flow with properties based on the

Table 1 Vortex generator dimensions

Configuration	b, in.	b_T, in.	c, in.	AR	θ, deg	S_a, in.²	S_g,[a] in.²
A1	0.25	0.25	1.000	0.25		0.250	0.250
2	0.25	0.25	0.500	0.5		0.125	0.125
3	0.25	0.25	0.250	1		0.063	0.063
4	0.25	0.25	0.125	2		0.031	0.031
5	0.50	0.50	1.000	0.5		0.250	0.500
6	0.50	0.50	0.500	1		0.125	0.250
7	0.50	0.50	0.250	2		0.063	0.125
8	0.50	0.50	0.125	4		0.031	0.063
B1	0.25	0.25	1.000	0.5	76.0	0.125	0.125
2	0.25	0.25	0.500	1	62.5	0.063	0.063
3	0.25	0.25	0.250	2	45.0	0.031	0.031
3	0.25	0.25	0.125	4	26.5	0.016	0.016
5	0.50	0.50	1.000	1	62.5	0.188	0.250
6	0.50	0.50	0.500	2	46.0	0.094	0.125
7	0.50	0.50	0.333	3	33.6	0.062	0.083
8	0.50	0.50	0.250	4	26.5	0.047	0.063
C1[b]	0.25	0.10	0.715	0.5		0.125	0.125
2	0.25	0.166	0.401	0.75		0.083	0.083
3	0.25	0.19	0.284	1		0.062	0.062
4	0.25	0.222	0.132	2		0.031	0.031
5	0.50	0.332	0.802	0.75		0.200	0.333
6	0.50	0.381	0.568	1		0.142	0.250
7	0.50	0.444	0.265	2		0.066	0.125
8	0.50	0.464	0.173	3		0.043	0.083

[a] $S_g = S_a + S_\infty$.
[b] $\epsilon = 11.85°$ for all C configurations.

average Mach number M_a. It was found from an earlier boundary-layer survey on a similar flat plate that M_a was 72% of the freestream value M_∞. Thus, for drag calculations, the flow was considered as two regions: the region extending $\frac{1}{4}$ in. from the plate was treated as uniform flow at $M_a = 3.58$, and in the remainder of the flow, $M_\infty = 4.86$ governed. A combination of existing engineering methods was used to calculate skin friction, base drag, drag due to lift (with zero thickness), and drag of the leading-edge wedge of each configuration, as follows.

The Reynolds number based on the mean geometric chord was used in determining the skin-friction coefficients. Since the boundary layer was itself turbulent, turbulent-flow coefficients were used in this region. For the sections of the longer-span vanes which extended into the freestream, the Reynolds numbers were generally below one million; here laminar friction coefficients were used. The turbulent-flow relation[5]

$$C_f/C_{fi} = (1 + 0.15\,M_a^2)^{-0.58} \tag{1}$$

was used in conjunction with Kármán-Schoenherr incompressible friction, and for laminar flow

$$C_f/C_{fi} = (1 + 0.045\,M_\infty^2)^{-1} \tag{2}$$

was used with Blasius incompressible coefficients.

Reference 5 gives base drag coefficients of 0.06 and 0.1 for the freestream and boundary-layer Mach numbers. These were converted from a base-area reference to planform area.

The drag component of the pressure forces on each vane at angle of attack (drag due to lift) was calculated using the flat-plate theory of Ref. 6. Thickness effects were considered separately and are discussed later. Linear theory was used, and for nearly half the vane configurations the flow was two-dimensional. Thus,

$$C_D = 4\alpha^2/(M^2 - 1)^{1/2} \tag{3}$$

For the rectangular and raked-tip planforms, the drag for the areas within the tip cone was one-half the corresponding two-dimensional value. One delta configuration (B1) had a subsonic leading edge and the drag coefficient found from Ref. 6 was 93% of the two-dimensional value. In all cases, the necessary adjustments for reference areas and the two-Mach number regimes were made.

The bluntness of the leading edge of a wedge can produce increased pressure on the wedge faces which may markedly increase the drag compared to a sharp wedge.[7-9] Viscous interaction may produce similar pressure increases. However, the relatively low Mach number and high Reynolds number of the present tests were such that the interaction was neglected in accordance with the conclusions of Ref. 7. The vane leading edge was treated as a flatly-truncated wedge, using the method of Chernyi.[9] The pressure along the wedge faces is influenced by the drag coefficient of the blunted nose C_{D_n}; this coefficient was calculated using Newtonian impact theory and measured values of vane bluntness.

The Chernyi expression for the pressure on the wedge faces is

$$P = \frac{P_\infty}{2}\left[\frac{(2)^{1/2}(\gamma+1)^{1/2}(\gamma-1)\gamma^{3/2}}{3(3\gamma-1)}\,C_{D_n}M_\infty{}^3\,\frac{d}{x}\right]^{2/3} \tag{4}$$

where d is the width of the nose bluntness, and x is the distance along the wedge axis. The total drag of the wedge of total angle ϕ is

$$D_w = D_n + 2\int_0^l p\,\tan(\phi/2)dx \tag{5}$$

where D_n is the drag of the blunt nose and the integral term gives the pressure drag on the two wedge faces. Chernyi's final expression for the drag coefficient of the wedge is shown in Ref. 8 to be in error, and the emended version is given as

$$C_{D_w} = [(\gamma+1)/4 + 4\gamma/t]\tan^2\alpha \tag{6}$$

where $t = (4l/dC_{D_n})\tan^3\alpha$. This is an approximation valid for large t, a restriction met by the vane configurations used. The derivation also presumes zero angle of attack; it was used herein for $\alpha = 5°$.

For one face of the wedge aligned with the flow,

$$C_{D_w} = [\gamma + 1 + (2\gamma/t)]\tan^2\alpha \tag{7}$$

In the present tests, the wedge half-angle was 11°, hence Eq. (7) was applied to the 10° and 15° angle-of-attack conditions.

Results

The results are shown in Fig. 2. The test data are shown by the symbols, and the solid curves are faired through the calculated results for each configuration tested. The upper half of each figure is for a span equal to the boundary-layer thickness ($b = \delta$), and the lower half is for $b = 2\delta$.

The agreement between the test and computed values is generally good. The major area of disagreement is for the shorter spans with low AR and higher α's. These configurations were physically small in planform area, and thus, the results were strongly influenced by experimental uncertainties and analytical approximations. The variation in test repeatability, for instance, was ±5% whereas for the larger configurations the variation was nearer ±1%. Over-all, the calculated values were 7.4% higher than the measured values; thus, the analytical method appears suitable for engineering design purposes.

Because of the variety of generator shapes and sizes, there were few general trends evident in the calculated components of drag. Skin friction was a minor contribution except for the larger planform areas at low α, where it approached 20% of the total. Base drag also approached 20% (for small planform areas and α's); this would be reduced even further by use of biconvex or double-wedge airfoil sections. Drag caused by lift was the major factor in 15% of the configurations, where the α's and planform areas were large. (The planform area did not influence the lift coefficient, but it reduced the wedge-drag coefficient contribution.) Thus the drag of the leading-edge wedge was predominant in 85% of the configurations. The average leading-edge bluntness was 0.004 in., and it does not appear feasible to reduce this appreciably except under laboratory conditions.

References

[1] Edwards, J. B., "Free-Flight Tests of Vortex Generator Configurations at Transonic Speeds," TN Aero. 2862 (AD 298824), Dec. 1962, Royal Aircraft Establishment, London.

[2] Mitchell, G. A. and Davis, R. W., "Performance of Centerbody Vortex Generators in an Axisymmetric Mixed-Compression Inlet at Mach Numbers from 2.0 to 3.0," TN D-4675, July 1968, NASA.

[3] O'Donnell, F. B. and Westkaemper, J. C., "Measurement of Errors Caused by Misalignment of Floating-Element Skin-Friction Balances," *AIAA Journal*, Vol. 3, No. 1, Jan. 1965, pp. 163–165.

[4] Whitten, J. W., "The Drag of Vane-Type Vortex Generators in Compressible Turbulent Flow," Rept. DRL-556 (AD 822140) Aug. 1967, Defense Research Laboratory, The Univ. of Texas at Austin, Austin, Texas.

[5] Hoerner, S. F., *Fluid Dynamic Drag*, 2nd ed., published by author, Midland Park, N. J., 1965, pp. 17–4, 16–11.

[6] Bonney, E. A., *Engineering Supersonic Aerodynamics*, McGraw-Hill, New York, 1950, pp. 136–159.

[7] Kendall, J. M., Jr., "An Experimental Investigation of Leading-Edge Shock-Wave Boundary Layer Interaction at Mach 5.8," *Journal of the Aeronautical Sciences*, Vol. 24, No. 1, Jan. 1957, pp. 47–56.

[8] Cramer, R. H., "Blunted Wedge Drag at Hypersonic Speed," BBA-RE-004-67, Applied Physics Laboratory, Johns Hopkins Univ., Baltimore, Md.

[9] Chernyi, G. G., *Introduction to Hypersonic Flow*, Academic Press, New York, 1961, p. 222.